

A summary of the PRUDENCE model projections of changes in European climate by the end of this century

Jens Hesselbjerg Christensen and Ole Bøssing Christensen

Danish Meteorological Institute, Denmark

Submitted to *Climatic Change*, Special Issue: PRUDENCE

Corresponding author:

Jens Hesselbjerg Christensen, Danish Meteorological Institute, Lyngbyvej 100, DK-2100

Copenhagen Ø, Denmark. jhc@dmi.dk

Abstract

An overview of the PRUDENCE fine resolution climate model experiments for Europe is presented in terms of their climate change signals, in particular 2-meter temperature and precipitation. A comparison is made with regard to the seasonal variation in climate change response of the different models participating in the project. In particular, it will be possible to check how representative a particular PRUDENCE regional experiment is of the overall set in terms of seasonal values of temperature and precipitation. This is of relevance for such further studies and impact models that for practical reasons cannot use all the PRUDENCE regional experiments. This paper also provides some guidelines for how to select subsets of the PRUDENCE regional experiments according to such main sources of uncertainty in regional climate simulations as the choice of the emission scenario and of the driving global climate model.

1. Introduction

An important issue when considering adaptation and mitigation responses to climate change is the uncertainty in the predictions of future climate. In addition to uncertainties derived from the model formulation there are those derived from natural climate variability and future atmospheric emissions. A single realisation of simulated climate is insufficient to provide the information needed for a comprehensive assessment of potential climate change and its impacts. This is already well recognised, with many atmosphere-ocean general circulation model (AOGCM) experiments involving ensemble integrations to provide a more exhaustive sample of possible future climates (*e.g.* Palmer and Räisänen (2002), Murphy *et al.* (2004) or Stainforth *et al.* (2004)). Similarly, the future anthropogenic forcing of climate is a function of uncertain socio-economic and technological developments, and various emissions scenarios have been developed to provide future climate forcing for AOGCM experiments.

However, neither of these issues has been addressed, to date, in the context of high-resolution climate change scenarios. The PRUDENCE project (Christensen *et al.*, 2006, this issue) has provided an initial evaluation of these uncertainties by running two atmosphere-only general circulation model (AGCM) ensembles and four regional climate model (RCM) ensembles and by using two different emissions scenarios to drive its simulations of future climate (see also Table 1).

A novel feature of PRUDENCE is its application of these high-resolution climate change scenarios as inputs to climate impact models, and the socio-economic interpretation of the results in relation to European policy making. –Conventionally, impact modellers have applied coarse resolution mean changes in climate, with some appropriate post-processing, to impact models calibrated using observed data (*e.g.* New *et al.*, 1999).

PRUDENCE has demonstrated an alternative approach in two areas. Firstly, it has provided high-resolution data, which are better suited as input to impact models; high spatial resolution provides a better description of orographic effects and land-sea contrast, and high temporal resolution in combination with high spatial resolution provides improved treatment of the physical and dynamical processes leading to extreme events like heavy precipitation. Secondly by applying climate model simulations for the present-day (control) period, during which climate observations are also available, impact modellers are able to assess the potential of using model outputs directly in climate change applications (*e.g.* Jacob *et al.*, 2006). This will provide more confidence in the use of atmospheric-forcing simulations across the full spectrum of spatial and temporal resolutions for estimating future climate impacts.

There is a clear need for a systematic evaluation of the current RCMs being applied in Europe, which involves not only an examination of the climate outputs from different models, but also estimations of the range of uncertainties that will propagate to impacts models. From the point of view of policy-relevant impact assessments, it is important to investigate the capability of RCMs in providing:

(a) More reliable estimates than GCMs of future *changes* in climate over the region and at the scale of interest based on the improved performance of RCMs in simulating present-day climate.

However, one should note that it is the case for both global and regional models, that establishing superior performance at the simulation of present-day climate may not be a sufficient indicator of the performance for future climate.

(b) Additional information on impact-relevant climate variables that GCMs cannot provide (*e.g.* on the severity and frequency of many weather extremes);

(c) Additional information on sub-GCM-grid scale uncertainties in projections.

Each of these items is thoroughly addressed in many of the papers in this special issue (see Christensen *et al.* (2006) for an introduction).

In this paper we provide an introduction to the PRUDENCE experiments and present a brief summary of the model climate change outputs. Detailed analyses of these results and their applications in impact assessment are discussed at length in other papers in the special issue. In Section 2 we briefly summarise the general model set-up and experimental design as it has been used within the PRUDENCE project. The quality of the models that participated in the PRUDENCE project in terms of their ability to simulate present day temperature and precipitation climate at the seasonal scale compared with the quality of the driving GCM is addressed by Jacob *et al.* (2006), so we will not focus on this aspect here. Instead, we build upon their conclusion that although some models appear to have relatively large systematic biases, the ensemble mean performs well.

Since the impact-related studies carried out within the PRUDENCE project are normally carried out through studies of individual model simulations, a clear need has been identified to compare the projected climate changes simulated by the individual models to the results of the whole suite of models applied. Section 3 summarises the projected climate change signals in temperature and precipitation as simulated with the PRUDENCE complete suite of model experiments, and can be compared to the more synthesised analysis on how this explores the uncertainty matrix due to model formulation and scenario generation provided by Déqué *et al.* (2006). Section 4 discusses the simulated changes in relation to the use of these models for impact studies, and Section 5 concludes this assessment.

2. Experimental set-up

At the time of the planning of PRUDENCE, high-resolution (horizontal grid-spacing up to 150 km) AGCMs were in preparation at European climate modelling centres. Atmospheric radiative forcing and matching sea-surface boundary conditions from coarse-resolution AOGCMs were set to drive them. The radiative forcing builds on the SRES A2 and B2 emission scenarios (Nakicenovic *et al.*, 2000). Simulations with the Hadley Centre high-resolution atmospheric GCM HadAM3H (Buonomo *et al.*, 2005) had already been conducted and determined the time window (1961-1990 and 2071-2100) adopted for the PRUDENCE experiments. Other experiments were also expected to become part of the PRUDENCE project (see Table 1). Four distinct sets of GCM experiments were conducted to form the basis of scenario generation and of an uncertainty analysis:

1. One ensemble using one AGCM with driving conditions (radiative forcing SRES A2 and matching sea-surface boundary conditions) from each of a three-member AOGCM ensemble (the HadAM3H atmospheric GCM with surface boundary conditions from 3 ensemble members of the coupled GCM HadCM3);
2. One ensemble using four different AGCMs with driving conditions (radiative forcing following SRES A2 and matching sea-surface boundary conditions) from the same AOGCM; (the HadAM3H, ECHAM5, ARPEGE, and NASA FVGCM AGCMs);
3. Two AGCMs (HadAM3H and ARPEGE) with driving conditions from two AOGCM experiments performed with the same AOGCM (HadCM3) but different atmospheric emissions (SRES B2 rather than A2);
4. One AGCM (ARPEGE) with driving conditions from two different AOGCMs using the same atmospheric emissions (A2).

Several of these models in turn provided lateral boundary conditions for the RCM simulations.

Several state-of-the-art European regional climate models were to be run using boundary conditions from two of the AGCMs mentioned. At the time of planning, eight models were participating. During the progress of the project two additional RCMs were included in the project and performed the “standard” experiment (point 1 below) in an intermediate resolution of about 50km. Five distinct experiments were conducted to provide the raw data for scenario generation and to further explore uncertainties, though other sensitivity studies were also performed in the PRUDENCE project:

1. Ten were driven by boundary conditions from one of the AGCM simulations (HadAM3H A2 emissions) taken from the three-member ensemble;
2. Two (HIRHAM and HadRM3H) were driven by boundary conditions from the 3 members of the one-model AGCM ensemble (HadAM3H with A2 emissions);
3. Five of these models (HIRHAM, HadRM3H, RegCM, RCAO, and PROMES) were also driven by the same AGCM, but forced by a different emissions scenario (B2 rather than A2);
4. The two-member AGCM ensemble using the same emissions scenario but a different AGCM than above was used to drive the stretched AGCM.
5. Two RCMs (HIRHAM and RCA2) performed the standard experiment in twice the original resolution, *i.e.*, around 25km instead of 50km. HIRHAM additionally performed the standard experiment in four times the original resolution, *i.e.*, around 12km.

The analysis reported here involves nine regional models and one stretched global model; the met.no version of HIRHAM has not been included. Results from a more recent version of the Hadley Centre RCM using a new set of AGCM boundary conditions were also made available. The experiments with this model does not differ substantially (Moberg and Jones, 2004) from those

using the original version, but we have decided to show all the results for reference. Finally, two sets of RCM experiments using an alternative driving GCM were added to the database.

We will here concentrate on the experiments using the original HadAM3H as the driving model and add a few additional experiments in order to investigate the additional level of uncertainty that is introduced when a different GCM is used as a driving model. Also, we only focus on the A2 experiment, as all models clearly show that the B2 experiment gives a relatively scalable result with a similar but weaker climate change signal as compared to the A2 experiments (Déqué *et al.*, 2005).

The time-slice experiments using HadAM3H were designed to provide the best possible present-day global climate using an atmosphere stand-alone model. It is well known that a GCM is better constrained towards the observed climate when sea surface temperatures and sea-ice conditions are specified according to the observed climate, rather than using the SSTs that could be generated from an experiment where the model is coupled to an ocean model. For this reason, the SSTs used in the control experiment were taken from a gridded data set of monthly mean observations covering the period 1960-1990, the HadISST dataset (Rayner *et al.*, 2003) - the actual individual months were used. Daily values were generated by interpolation between succeeding months.

All analyses of the simulations have been performed on the period 1961-1990, allowing for models to spin-up their surface variables during the first model year. The climate change experiment used SSTs from an existing HadCM3 simulation in the following way: First the anomaly fields with respect to the AOGCM control 30 year monthly mean climatology for each individual month in the scenario period (representing 2071-2100) were constructed. These anomalies were then added to the 30 year averaged gridded monthly mean observed climatology. This way the inter-annual variability of scenario SSTs reflects those in the coupled AOGCM, while the SSTs used during the control

period reflects those observed. All experiments that have been based on the Hadley Centre 3rd generation models (HadCM3 and HadAM3) have basically used this set-up.

In the Swedish RCAO model the approach is somewhat different, as it includes a coupled regional ocean model for the Baltic Sea that internally generates its own SSTs in that area. The SSTs from RCAO have been used in RACMO, in the HIRHAM 12km simulation, and in the high-resolution version of RCA that is run as an atmospheric stand-alone experiment. This set of 9 RCMs is referred to as the PRUDENCE standard experimental set-up.

Two additional AOGCMs used as driving models will also be discussed in the following. We therefore briefly discuss the set-up of these experiments.

Two of the RCMs have also been used for experiments with boundary conditions from the ECHAM4/OPYC3 model (Roeckner *et al.*, 1996). In this set-up a more traditional procedure was used. The atmospheric boundary conditions as well as the SSTs were taken directly from the driving GCM; no use of an intermediate high resolution AGCM was made. It should be noted that the scenario time slice for the two ECHAM4/OPYC3-driven experiments (RCAO and HIRHAM) used two different realisations of this experiment. In addition, results are shown from an experiment with the stretched ARPEGE model using both the standard PRUDENCE set-up as well as SSTs from an experiment using a coarser-resolution (non-stretched) ARPEGE version coupled to the OPA ocean model. In this case the SSTs used were processed as described above in the standard PRUDENCE set-up.

References for the nine regional models as well as the French ARPEGE model and the second version of the Hadley Centre RCM, that we have chosen to include in the present analysis are the

following (see also Table 1): ARPEGE (Gibelin and Déqué 2003); CHRM (Vidale *et al.*, 2003); CLM (Steppeler *et al.*, 2003); HadRM3H and HadRM3P (Buonomo *et al.*, 2005; Jones *et al.*, 1995); HIRHAM (Christensen *et al.*, 1996); PROMES (Castro *et al.*, 1993); RACMO (Lenderink *et al.*, 2003); RCAO and RCA2 (Jones *et al.*, 2004; Meier *et al.*, 2003; Döscher *et al.*, 2002); RegCM (Giorgi and Mearns 1999), and REMO (Jacob, 2001). A brief summary of each of the models can be found in Déqué *et al.* (2006)

3. Projected climate change

Figures 2ab and 3ab summarise the overall PRUDENCE projections of change for each of the models under investigation and for summer and winter. For brevity we do not show spring and autumn, although we will comment on these as well. In Figure 1 the arrangement of panels in these summaries is explained. The panels will be referred to by coordinates in the text.

This compilation of seasonal “postage stamps” is organised as follows (compare with Figure 1): in each figure the present-day climate (CRU 1961-1990; New *et al.*, 1999) is shown for reference in panel 1A (a separate label bar is also inserted). The multi-model ensemble mean over a maximum overlap domain of the standard PRUDENCE RCM experiment (driven by the HadAM3H AGCM) is shown in panel 1C, while the inter-model standard deviation of the quantity shown is in panel 1D.

Row 2 is organised to include information about the two Hadley Centre driving AGCMs and corresponding RCM experiments. In column A the results are from the driving model used for the standard PRUDENCE RCM experiment (driven by the HadAM3H AGCM), while column B shows the results from the corresponding Hadley RCM. Column D shows the results from a revised version of the Hadley Centre AGCM called HadAM3P, which was introduced during the course of the project, while column C holds information from the corresponding Hadley RCM (HadRM3P), such that the regional results of columns B and C can be easily compared. A substantial amount of

impact-related work has been carried out outside the PRUDENCE project based on Hadley Centre RCM results from HadRM3P rather than HadRM3H, which is maintained in PRUDENCE for reference purpose, to keep the experiment and analysis clean.

The following two rows, 3 and 4, show the results from the individual model simulations for the standard PRUDENCE RCM experiments (driven by the HadAM3H AGCM). Each model group and experiment can be identified from Figure 1, enclosed by the thick black boundary. In a few cases more than one realisation of the downscaling experiment was conducted (HadRM3H and HIRHAM). In this case only results from the first (standard) ensemble member are shown

Immediately below the standard PRUDENCE RCM experiments, results from two additional experiments with doubled resolution (25km instead of 50km) in RCAO/RCA2 and HIRHAM are shown (panels 5C and 5D). This facilitates assessment of the added value due to resolution.

Furthermore, below the HIRHAM 25km experiments in panel 6D, are shown results from a 12km experiment with the same model. Note that the HIRHAM 25km simulation uses the standard SST/Sea ice values, whereas the 12km simulation uses fields from the RCAO model over the Baltic Sea.

Panels 7C and 7D contain another set of identical experiments with the same two RCMs that have been conducted taking boundary conditions from a different AOGCM, in this case the AOGCM ECHAM4/OPYC3 from the Max-Planck Institute of Meteorology.

The plot in panel 6A shows the climate change signal from the underlying coupled AOGCM (HadCM3) experiment used to design standard PRUDENCE time-slice experiments. Finally, panels 6B and 7B show the results from the stretched ARPEGE model. Panel 6B shows results from the

standard PRUDENCE set-up, while a different set of sea surface temperatures (from a coupled ARPEGE/OPA simulation) was used to force the second experiment in panel 7B.

Changes in large-scale weather patterns as represented in the high resolution experiments are mostly due to the driving model simulation (see also Déqué *et al.* 2006). This is clearly seen for both temperature and precipitation when comparing the HadAM3H-driven results with the RCM results driven by ECHAM4/OPYC3 (panels 7C and 7D). The ARPEGE simulation (6B) also deviates from the other GCM experiments. In particular, it can be seen in the North Atlantic that there is a much larger warming and precipitation increase during winter in the ECHAM4/OPYC3-driven simulations.

Temperature change

The standard HadAM3H-driven simulations exhibit warming everywhere in all seasons. When compared to the ECHAM4/OPYC3-driven experiments (7C and 7D), warming over the Atlantic Ocean is generally smaller. Continental warming is influenced by this more moderate oceanic warming, such that *e.g.* warming over the British Isles is considerably reduced in winter in the HadAM3H-driven experiments compared to those driven by ECHAM4/OPYC3. At the same time, the ECHAM4/OPYC3 has a clearer tendency for strong warming in southern Europe in summer.

Winter

Figure 2a shows a remarkable agreement among the HadAM3H-driven experiments in the projected temperature change across the model domain with major excursions from the ensemble mean value related to the snow and ice covered areas in the east and north. In the Atlantic sector, all models in the standard set-up agree within less than 0.5 °C, largely controlled by the warming over the Atlantic Ocean. When comparing the RCMs with the driving AGCM (2A) and the underlying

AOGCM (6A) it is clear that the projected warming by the RCMs is generally less, particularly in the snow covered region.

The higher-resolution simulations (5C, 5D, 6D) generally do not show any significant differences with respect to their coarser-resolution counterparts. However, when driven by a different GCM (ECHAM4/OPYC3; 7C and 7D) the RCMs show a different warming pattern, rather consistent between the two RCMs used; the difference between the warming patterns is partly due to the fact that the scenario boundary conditions belong to two different realisations. The two ARPEGE experiments (6B and 7B) agree relatively well.

The inter-model standard deviation (1D) reflects that sea temperatures are prescribed; the spread increases eastwards away from the ocean.

Spring

This is basically a repetition of the situation discussed for winter (not shown). The warming is largest over areas where snow cover retreats, and the same systematic inter-model differences are observed. It is noted that in the ECHAM4/OPYC3-driven experiments, a tendency for the RCAO model to warm more in the south than in HIRHAM is seen; again the different scenario boundaries should be kept in mind, however.

Summer

Figure 2b differs considerably from the other seasons. There is a much wider spread of projected changes, which is due to the different formulations of the models. However, the general trend that the warming is reduced with increased resolution is even clearer in this season. The higher-resolution experiments (5C, 5D, 6D) exhibit reduced warming in the south when compared to their

standard resolution counterparts. The RCAO/RCA2 model is warmer than HIRHAM in both the standard PRUDENCE experiment and the ECHAM4/OPYC3-driven experiments.

The HadCM3-projected warming (6A) over the Baltic Sea is very large. A significant contribution to this is a too cold control period (monthly means averaged over the Baltic Sea are 4-8K lower than observed for JJA (Kjellström *et al.*, 2005) in the low-resolution coupled simulation. The Baltic Sea is particularly difficult to model in low resolution due to the very narrow outflow region. In fact, the Baltic Sea is not connected to the North Sea in the underlying HadCM3. RACMO (3D) , with SSTs from RCAO, and RCAO (4C) show the least warming over the Baltic model of all the RCMs

Finally, all models agree that the largest warming is projected to occur in the Mediterranean region, and most of the models point towards southern France and the Iberian Peninsula as being the region most severely hit by this warming of more than 6°C. Both of the ARPEGE experiments (6-7B) show relatively less warming compared to most of the RCMs, with the OPA-driven one (7B) giving the lowest warming in Southern Europe.

The standard deviation (1D) is larger than other seasons, reflecting that the role of the RCM is larger during summer where weather to a high extent is locally generated. In particular, the amount of evaporative cooling of the surface in dry summer conditions depends on the surface scheme used by the regional model.

Autumn

In this season (not shown) there is little variability across the models, except with the general tendency that warming is reduced going from AOGCM via AGCM to RCM with a hint towards a

further reduction going from standard resolution to higher resolution. There is a large-scale warming across the entire region of approximately 4°C almost uniformly everywhere.

The strong warming of the Baltic Sea seen in summer is notable also during autumn, again with exceptions in RCAO and RACMO. The RCM experiments with ECHAM boundary forcing also look similar in this case, with HIRHAM a little warmer than RCAO, and again a fairly uniform warming, in this case of 5-6°C. Once again the OPA-driven ARPEGE experiment shows the least warming of all experiments.

Precipitation

Like most other GCM climate change simulations, the HadAM3H experiment shows a north-south gradient in projected European precipitation change with positive changes in the north and negative changes in the south. However, the line of zero change moves with the season.

Winter

Figure 3a clearly depicts the feature that a general increase in the north changes to a decrease in the far south. In relative terms all the models depict this pattern quite systematically and the patterns of change are similar across all the standard PRUDENCE simulations. Details of the transition from reduction to increase vary between the models, as is also inferred from the standard-deviation diagram in panel 1D. The relatively largest spread is found over this transition zone.

The resolution aspect is not obvious in this case, as winter precipitation changes to a large degree follow changes in the general atmospheric circulation. Little is changed going from the HadAM3H simulation (2A) to any of the RCMs –the large scale control on the simulations dominates the result. Moreover, only marginal changes are seen between the high-resolution simulations (5C-D

and 6D) and their standard counterparts (4C-D). The difference between the HadCM3 (6A) and HadAM3H (2A) cannot be attributed to resolution only, but also to different dynamical responses.

There is a reduction in precipitation in Norway in the standard HadAM3H-driven experiments. This is attributed to a lee effect connected to a more south-westerly flow in the future scenario. This reduction in precipitation is stronger in the regional models than in the driving model and serves as an example of larger-scale changes influenced by resolution.

For the ECHAM-driven experiments 7C-D, the pattern of largest increases in the north is replicated. However, a much larger increase is observed in Northern Europe; the reduction in precipitation in Norway is absent in the ECHAM-driven experiments. The ARPEGE experiment driven by OPA (7B) exhibits the smallest change of all the experiments shown.

Spring

This season (not shown) mimics what was stated above for winter. The transition line between positive and negative climate change is further to the north than during winter. The major difference is observed between the two ECHAM-driven experiments: Also in this season, the RCAO model has a larger response than HIRHAM.

The standard deviation is more diffuse, consistent with the transition from large-scale governed winter and locally generated summer weather.

Summer

Figure 3b is the equivalent of Figure 2b in many aspects. There is a much wider spread between the simulated changes from model to model. This is reflected by the inter-model standard deviation

(1D; shown in this figure with a different scaling than in the others), which is much larger than for the other seasons. The largest spread is found over the Mediterranean Sea and over the Baltic Sea. The latter is related to the very warm SST anomalies in the HadCM3 simulation that also affects many of the RCMs. Most RCMs tend to have quite different detailed responses to this, while the RCAO and RACMO models (4C and 3D) deviate, largely due to the specification of SSTs from the RCAO Baltic Sea ocean component; see Kjellström and Ruosteenoja (2006, this volume).

When comparing the two 25km experiments (5C-D) and the 12km experiment (6D) with their lower-resolution counterparts (4C-D), it appears that the higher-resolution experiments show less of a tendency to become drier, and the increase in precipitation in the north is further enhanced. A similar RCM dependence of the pattern of change is seen in the ECHAM-driven experiments, again with the RCAO model (7C) showing a much larger response than HIRHAM (7D). The two ARPEGE experiments (6-7B) are comparable, except over the Baltic Sea.

Autumn

For autumn (not shown) a similar impression as for spring is given. There is little overall change in comparison to winter and summer, whereas a clear reduction is now simulated over the Iberian Peninsula. In the south-east there is a large inter-model standard deviation. Locally, even the sign of change may differ. However, this is the driest part of the region with very small present-day precipitation. The large scale agreement is even more interesting, as it is also found in the ECHAM-driven experiments as well as in both ARPEGE simulations. For the ECHAM-driven runs the effect of a different large scale circulation change than in HadAM3H is responsible for a somewhat larger increase in the north. Resolution seems not to be dominant in this season, though there seems to be more positive changes with increased resolution.

As a complementary illustration of the relative magnitude of the climate change of the respective models, we have divided the European area into sub-areas as indicated in Figure 4. In Figure 5 we show area averages over these areas from the respective regional models. The numbers in Tables 2 and 3 correspond to the colours plotted in Figure 5. Here the results for spring and autumn are also shown.

4. Discussion

While it would be a very interesting exercise to address the origin of the individual model differences, this goes beyond the scope of the present paper which is meant to portray the broad inter-model differences mostly for the purpose of informing users of the features of the PRUDENCE model results. We shall propose ways to select model experiments to represent the spread among simulations, for instance for the case where impacts modellers aim to use input representing the model variability, but where it is not possible to use the entire set.

Based on this collection of RCM and GCM experiments it is possible to start investigating the effects on impact modelling of the choice of emission scenario, global model, regional model, resolution or ensemble member. Indeed, it has been a central objective of the PRUDENCE project to put initial quantitative measures on the uncertainty associated with these choices (see *e.g.* Christensen *et al.*, 2006). In order to sample these aspects with a minimal subset of model experiments, selections of PRUDENCE RCM experiments for impact analyses can be based on one or more of the following possibilities:

1. The role of the driving GCM versus the downscaled RCM
2. Same driving GCM, different RCMs (minimum)
3. Same driving GCM, different RCMs (complete set)
4. Same RCM, different driving GCMs

5. Same RCM and GCM, different emission scenarios
6. Same RCM, GCM, and emission scenario, different ensemble members
7. Same driving GCM and RCM, different resolution of RCMs
8. Same RCM, different parameterizations
9. Same GCM and RCM combination with comparable/different physics parameterizations

Actual selections could be: Set 1 fulfilling criteria 1, 2, 4, and 5: HadAM3H, ARPEGE, all HIRHAM and RCAO 50km A2 experiments, and REMO, supplemented by the HIRHAM and RCAO HadAM3H-driven B2 experiments. Set 2 fulfilling criteria 6, 7, 8, and 9: HadRM3H and HadRM3P, and HIRHAM in all resolutions. Or set 2 extended by set 3 to fulfil criterion 3: CHRM, CLM, PROMES, and RegCM. These sets have already been recommended for impacts analyses during the PRUDENCE project. Note that PROMES and RegCM are more limited in their application for impact assessment because of their truncated domain over Northern Europe.

As an additional parameter in the choice of models, the climate sensitivity could be selected. Figure 4 can act as a guide here. It is obvious that no model deviates from the overall set for both fields and all seasons. Rather, the choice of driving models depends on the field and season under investigation. As an example, the Hadley Centre models seem to have a very high sensitivity with respect to summer warming; for summer precipitation changes it is roughly in the middle of the pack, however. Conversely, the CHRM model exhibits rather average summer warming while having the largest relative reductions in summer precipitation. The RCAO model in both resolutions exhibits the largest summer warming after the Hadley Centre models. The ECHAM4/OPYC3-driven models are seen to have much larger precipitation increases than the HadAM3H-driven ones in the northern SC area, and they also show a much stronger warming.

Running through the list of models we see the following:

HadAM3H shows large warmings for all regions, except for autumn. During summer the precipitation decrease is on the strong side.

HIRHAM driven by HadAM3H is quite in the middle of the range for most areas, fields and seasons, with a lesser drying during summer than average. It also has a slight tendency to less warming and a more positive precipitation change (in particular during summer) with increased resolution.

CHRM shows a rather small warming, especially during autumn with values at times more than half a degree lower than the ensemble mean. At the same time it shows a very large reduction in precipitation during summer.

CLM is similar to CHRM with respect to temperature changes, showing lower warming during autumn. Precipitation change is average.

HadRM3H shows warming and precipitation changes very similar to HadAM3H.

RegCM does not cover the Scandinavia region (SC). For the rest of the areas its performance is similar to the ensemble average for both temperature and precipitation; Southern Europe precipitation decrease is slightly less than average.

RACMO is close to the average, except for large summer warming in MD and precipitation decrease in the southern regions (IP, AL, MD, and EA).

REMO exhibits a larger winter warming in Northern and Eastern Europe, but a smaller summer warming over most regions. It has an increase in summer precipitation in SC, probably because the large Baltic Sea warming reaches further inland than is the norm, due to the mosaic description of the land-surface scheme.

RCAO shows a rather large warming in summer in Southern Europe (IP, FR, and AL, MD). In the SC area the incorporated Baltic Sea model tends to reduce the warming relative to the atmosphere-only regional models (see Figure 2b). Similarly to the HIRHAM model, the effect of even higher resolution is slight and towards more positive precipitation changes and a reduction in warming.

PROMES, like RegCM, does not cover SC. During spring it is warmer than most models, but is closer to the ensemble mean in summer. During summer a small precipitation reduction is seen over EA, like REMO, and over AL in autumn. while most models have a reduction

ARPEGE, like HIRHAM and RCAO with ECHAM boundaries, shows the biggest deviation from the PRUDENCE standard simulation and hence from the ensemble mean value. As these are based on different GCMs (ARPEGE is a stretched AGCM) this is not surprising and confirms that in most seasons and in most regions the choice of GCM is more important for simulated seasonal temperature and precipitation changes than the choice of RCM (see also Déqué *et al.*, 2006, this issue). This is also suggested by looking at the two ECHAM4/OPYC3-driven RCM experiments. The systematic differences between these are rather similar to those between the same pair of RCMs in the standard PRUDENCE run.

5. Conclusion

The PRUDENCE collection of regional climate change simulations has been analysed through quantitative descriptions of each individual model with respect to climate change. This paper is a supplement to the validation of the models in Jacob *et al.* (2006, this issue) and to the analysis of sources of variability in Déqué *et al.* (2006, this issue). The purpose of this paper is to offer an overview of how the simulated changes vary among the PRUDENCE models and how each of these compare to the overall RCM ensemble mean..

Through a brief description of the characteristics of each model with respect to changes in 2-meter temperature and in precipitation at the seasonal scale, we have provided tools for impacts analysts to pick subsets of the PRUDENCE ensemble for further modelling. Which models fulfil similar criteria like the choice of driving model and of emission scenario is also explained. It should be noted, however, that the PRUDENCE collection of experiments is not exhaustive, since one particular global experiment, the HadAM3H model following the A2 scenario, provided boundary conditions for the bulk of the experiments.

With the help of Figs 2-3 and 5, a rough assessment can be made of the relative importance of driving model and regional model formulation in the numerical results. It can be seen that the driving model has a dominant effect on temperature during spring, winter, and autumn, which seems to be larger than the effect of the specific choice of regional model. The driving model is also important during summer, though the regional model has a larger role in this season. Regarding precipitation, the driving model seems to be relatively most important in spring and summer. These conclusions are in agreement with the more systematic treatment in Déqué *et al.* (2006, this issue).

The relative importance of the driving model may be larger than is shown in this paper, since the ECHAM4/OPYC3 and HadCM3 models are rather similar in their global climate change (IPCC, 2001).

Higher resolution of course gives higher orographic detail in the fields modelled. But there is also seen a tendency for less warming in the present model results. For HIRHAM, this is connected to a marginally lower atmospheric humidity in the high-resolution model, and hence a lower greenhouse effect. However, this could be due to the fact that the model physics has not been extensively tuned to the higher resolution, but rather taken directly from the lower-resolution standard parameterization.

It is noteworthy that regional models with quite different biases (Jacob *et al.*, 2006, this issue) are much closer to one another in simulating climate change. As an example, the temperature bias (Jacob *et al.*, 2006, Table 3.1.3a) of the SC area (Scandinavia) varies between 1.27 (HIRHAM) and 3.46 (REMO) in winter for the HadAM3H-driven regional models. The corresponding climate change (Table 2) varies between 3.68 (RACMO) and 4.67 (REMO), *i.e.*, within a range of half the bias range. For precipitation, summer biases for FR (France) vary between -47% (CHRM) and +0.51% (RegCM), (Jacob *et al.*, 2006, Table 3.1.4b), whereas climate change signals are between -55% (CHRM) and -34% (HIRHAM). The observed summer precipitation in the FR region is 1.84mm/day. The relation between model reference field biases and climate change signals, and the observation that the PRUDENCE models agree well on climate change when considering model bias, is made in a systematic treatment by Déqué *et al.*, (2005)

The bias of the selection of RCM experiments in PRUDENCE towards being driven by the HadAM3H A2 simulation has precluded a robust estimation of uncertainties in regional climate

change projections according to their source. A more systematic choice of RCM experiments with a variety of emission scenarios and global models is underway in the ENSEMBLES¹ project. In addition, these RCM experiments will cover the period 1950 to 2050 (some even continuing to 2100) instead of the two 30-year time slices treated in the PRUDENCE project. Hence, the analysis of PRUDENCE results will in the future be developed and enhanced through the ENSEMBLES project.

Acknowledgments

The authors would like to thank for financial support from the European Union through the PRUDENCE project (EVK2-CT-2100-00132). Important comments from several PRUDENCE participants, in particular Tim Carter, Markku Rummukainen, and Erik Kjellström, improved the manuscript greatly. We acknowledge the contributions from all participating institutions that delivered data for this work.

References

Buonomo, E., Jones, R.G. , Huntingford, C. and Hannaford, J.: 2005, The robustness of high resolution predictions of changes in extreme precipitation for Europe Q. J. R. Meteorol. Soc., in press.

Christensen, J. H., T. R. Carter, and M. Rummukainen, 2006: Evaluating the performance and utility of regional climate models: The PRUDENCE project, *Climatic Change*, this issue

Déqué, M., R. G. Jones, M. Wild, F. Giorgi, J. H. Christensen, D. C. Hassell, P.L. Vidale, B.

Rockel, D. Jacob, E. Kjöllström, M. de Castro, F. Kucharski, and B. van den Hurk, 2005: Global

¹ ENSEMBLES (Ensemble-based Predictions of Climate Changes and their Impacts) is a 5-year Integrated Project, 2004-2009, supported by the European Commission's 6th Framework Programme. See Hewitt and Griggs (2004).

high resolution versus Limited Area Model climate change projections over Europe: quantifying confidence level from PRUDENCE results, *Clim. Dyn.*, DOI 10.1007/S00382-005-0052-1.

Déqué, M., D. P. Rowell, D. Lüthi, F. Giorgi, J. H. Christensen, B. Rockel, D. Jacob, E. Kjellström, M. de Castro, and B. van den Hurk, 2006: An intercomparison of regional climate simulations for Europe: assessing uncertainties in model projections, *Climatic Change*, this issue

Döscher, R., U. Willén, C. Jones, A. Rutgersson, H. E. M. Meier, U., Hansson, and L. P. Graham, 2002: The development of the coupled regional ocean-atmosphere model RCAO. *Boreal Env. Res.* **7**, 183-192.

Hewitt, C.D and Griggs, D.J., 2004: Ensembles-based predictions of climate changes and their impacts. *Eos*, **85**, 566.

IPCC, 2001: Climate Change 2001: The Scientific Basis, Contribution of Working Group I to the Third Assessment Report of the Intergovernmental Panel on Climate Change [Houghton, J. T., *et al.*, (eds.)]. Cambridge University Press, Cambridge, United Kingdom and New York, NY, USA, 881 pp.

Jacob, D., L. Bärring, O. B. Christensen, J. H. Christensen, M. de Castro, M. Déqué, F. Giorgi, S. Hagemann, M. Hirschi, R. Jones, E. Kjellström, G. Lenderink, B. Rockel, E. Sánchez, C. Schär, S. I. Seneviratne, S. Somot, A. van Ulden, B. van den Hurk, 2006: An inter-comparison of regional climate models for Europe: Design of the experiments and model performance *Climatic Change*, this issue

Jones, R.G., J.M. Murphy, and M. Noguer: 1995: Simulation of climate change over Europe using a nested regional-climate model I: Assessment of control climate, including sensitivity to location of lateral boundaries, *Q. J. R. Meteorol. Soc.*, **121**, 1413-1449.

Jones, C. G., U. Willén, A. Ullerstig, and U. Hansson, 2004: The Rossby Centre Regional Atmospheric Climate Model Part I: Model Climatology and Performance for the Present Climate over Europe. *Ambio*, **33**, 199-210.

Kjellström, E., and K. Ruosteenoja, 2005: Present-day and future precipitation in the Baltic Sea region as simulated in a suite of regional climate models. *Climatic Change*, this issue.

Kjellström, E., R. Döscher, and M. Meier, 2005: Atmospheric response to different sea surface temperatures in the Baltic Sea: Coupled versus uncoupled regional climate model experiments. *Nordic Hydrology*, to appear in Vol.**36**(4).

Meier, H.E.M., R. Döscher, and T. Faxén, 2003: A multiprocessor coupled ice-ocean model for the Baltic Sea. Application to the salt inflow. *J. Geophys. Res.* **108**, C8, 3273.

Moberg, A., and P. D. Jones, 2004: Regional climate model simulations of daily maximum and minimum near-surface temperatures across Europe compared with observed station data 1961–1990. *Clim. Dyn.* **23**, 695–715.

Murphy, J. M., D. M. H. Sexton, D. N. Barnett, G. S. Jones, M. J. Webb, M. Collins, and D. A. Stainforth, 2004: Quantification of modelling uncertainties in a large ensemble of climate change simulations. *Nature* **430**, 768-772.

Nakicenovic, N., J. Alcamo, G. Davis, B. de Vries, J. Fenhann, S. Gaffin, K. Gregory, A. Grübler *et al.*, 2000: Emission scenarios. A Special Report of Working Group III of the Intergovernmental Panel on Climate Change. Cambridge University Press, 599 pp.

New, M., M. Hulme, and P. Jones, 1999: Representing Twentieth-Century Space–Time Climate Variability. Part I: Development of a 1961–90 Mean Monthly Terrestrial Climatology. *Journal of Climate* **12**, 829–856

Palmer, T. N., and J. Räisänen, 2002: Quantifying the risk of extreme seasonal precipitation events in a changing climate. *Nature* **415**, 512-514.

Rayner, N.A., Parker, D.E., Horton, E.B., Folland, C.K., Alexander, L.V., Rowell, D.P., Kent, E.C., Kaplan, A., 2003. Global analyses of SST, sea ice and night marine air temperature since the late nineteenth century. *J. Geophys. Res.*, **108** (D14), 4407, doi:10.1029/2002JD002670, 2003.

Roeckner, E., K. Arpe, L. Bengtsson, M. Christoph, M. Claussen, L. Dümenil, M. Esch, M. Giorgetta, U. Schlese, and U. Schulzweida, 1996: The atmospheric general circulation model ECHAM-4: Model description and simulation of present-day climate. MPI Report **218**, 90 pp., Max-Planck-Institut für Meteorologie

Stainforth, D. A., T. Aina, C. Christensen, M. Collins, N. Faull, D. J. Frame, J. A. Kettleborough, S. Knight, A. Martin, J. M. Murphy, C. Piani, D. Sexton, L. A. Smith, R. A. Spicer, A. J. Thorpe, and M. R. Allen, 2004: Uncertainty in predictions of the climate response to rising levels of greenhouse gases. *Nature* **433**, 403-406.

Tables

Table 1 Existing RCM and stretched-GCM (ARPEGE) scenario experiments in PRUDENCE. For ARPEGE, the numbers refer to SST and sea ice from HadCM3, as also used by HadAM3H, and SST and sea ice from the ARPEGE/OPA coupled GCM, respectively

	SRES scenario	HIRHAM	CHRM	CLM	HadRM3H	HadRM3P	RegCM	RACMO	REMO	RCAO	PROMES	ARPEGE stretched
HadAM3H, HadCM3	A2	3	1	1	3	3	1	1	1	1	1	3
ECHAM4/OPYC3	A2	1								1		
ARPEGE/OPA	A2											1
HadAM3H, HadCM3	B2	1			1		1			1	1	1
ECHAM4/OPYC3	B2	1								1		
ARPEGE/OPA	B2											3

Table 2 Change in seasonal mean 2-meter temperature for the 8 areas under investigation

DJF	BI	IP	FR	ME	SC	AL	MD	EA
HIRHAM-50	1.90	3.13	2.79	3.45	4.23	3.54	3.93	4.57
HIRHAM-25	1.71	3.05	2.70	3.24	4.15	3.49	3.69	4.26
HIRHAM-12	1.78	3.05	2.72	3.20	3.91	3.61	3.74	4.27
CHRM	1.52	2.46	2.31	2.67	3.86	3.03	3.08	3.80
CLM	1.72	2.64	2.50	3.03	3.68	3.40	3.46	4.14
HadRM3H	2.09	3.44	3.15	3.67	4.25	4.20	4.20	4.71
RegCM	1.82	2.73	2.52	3.13		3.22	3.70	4.28
RACMO	1.81	3.08	2.89	3.20	3.68	3.53	3.74	4.17
REMO	1.90	3.12	3.09	3.67	4.67	3.89	3.83	4.85
RCAO-50	1.83	3.06	2.78	3.31	4.19	3.50	3.60	4.46
RCAO-25	1.86	3.09	2.92	3.62	4.10	3.60	3.73	5.02
PROMES	1.84	3.05	2.78	3.15		3.49	3.61	3.91
HadAM3H	2.08	3.59	3.19	3.66	4.51	4.21	4.41	4.86
ARPEGE	1.96	3.05	2.71	3.05	4.75	3.10	3.32	4.04
HIRHAM-ECH	3.38	3.90	3.89	4.09	5.59	4.50	4.22	4.81
RCAO-ECH	3.28	4.15	4.34	4.98	5.82	5.07	4.30	6.06
Ensemble	1.83	2.97	2.76	3.25	4.08	3.53	3.68	4.32

MAM	BI	IP	FR	ME	SC	AL	MD	EA
HIRHAM-50	2.06	3.46	2.35	2.58	4.09	3.00	3.39	3.03
HIRHAM-25	1.94	3.34	2.20	2.42	3.84	2.88	3.15	2.81
HIRHAM-12	1.87	3.36	2.13	2.32	3.78	2.87	3.12	2.72
CHRM	1.79	3.05	2.28	2.50	3.65	2.94	3.02	2.96
CLM	1.95	2.87	2.30	2.61	4.33	3.14	2.89	2.96
HadRM3H	2.50	3.98	3.11	3.53	4.54	4.04	4.08	4.15
RegCM	2.15	3.28	2.74	3.26		3.42	3.30	3.63
RACMO	2.17	3.60	2.66	2.97	3.82	3.33	3.50	3.39
REMO	2.03	3.43	2.48	2.73	3.94	3.14	3.21	3.08
RCAO-44	2.03	3.35	2.52	2.97	3.69	3.17	3.26	3.44
RCAO-25	2.10	3.41	2.62	2.99	3.80	3.22	3.32	3.56

PROMES	2.25	3.73	2.99	3.28		3.68	3.64	3.82
HadAM3H	2.49	4.09	3.11	3.57	4.68	4.02	4.12	4.11
ARPEGE	1.86	3.61	2.63	2.96	3.35	3.45	3.86	4.40
HIRHAM-ECH	3.80	5.08	4.67	4.63	5.21	5.30	4.69	4.59
RCAO-ECH	3.88	5.99	5.34	5.00	4.68	5.69	4.68	4.76
Ensemble	2.10	3.42	2.60	2.94	4.01	3.32	3.37	3.38

JJA	BI	IP	FR	ME	SC	AL	MD	EA
HIRHAM-50	3.04	5.38	5.05	4.06	3.00	4.72	5.28	4.38
HIRHAM-25	2.86	5.27	4.77	3.76	2.74	4.48	5.06	3.89
HIRHAM-12	2.72	5.19	4.47	3.41	2.68	4.23	4.85	3.43
CHRM	2.79	4.90	4.71	3.59	2.32	4.83	4.85	3.71
CLM	3.18	5.00	4.90	3.71	2.58	4.44	4.51	3.50
HadRM3H	3.70	5.70	6.44	5.39	4.10	6.31	6.27	5.68
RegCM	2.96	4.93	4.79	3.82		4.60	5.02	3.66
RACMO	2.90	5.83	4.81	3.77	2.85	5.12	6.07	4.39
REMO	2.67	5.42	4.11	3.09	3.08	4.08	4.73	3.19
RCAO-44	2.98	5.73	5.93	4.64	2.91	5.82	5.94	4.66
RCAO-25	2.93	5.59	5.63	4.45	2.70	5.74	5.60	4.37
PROMES	3.19	5.82	5.45	4.38		5.42	5.83	4.69
HadAM3H	3.62	6.30	6.79	5.42	3.96	6.54	7.03	5.94
ARPEGE	2.29	4.78	4.51	3.76	3.25	5.05	5.52	4.84
HIRHAM-ECH	4.51	6.73	7.20	5.95	4.10	6.65	6.63	6.01
RCAO-ECH	4.51	7.83	9.01	7.11	3.17	8.55	7.57	6.80
Ensemble	3.05	5.41	5.13	4.05	2.98	5.04	5.39	4.21

SON	BI	IP	FR	ME	SC	AL	MD	EA
HIRHAM-50	3.17	4.12	4.20	4.17	4.72	4.54	4.43	4.61
HIRHAM-25	3.07	3.98	3.97	3.90	4.56	4.36	4.31	4.23
HIRHAM-12	3.01	3.96	3.91	3.87	4.50	4.32	4.20	4.14
CHRM	2.80	3.48	3.37	3.33	3.87	3.67	3.66	3.41
CLM	2.82	3.53	3.23	3.27	4.30	3.56	3.66	3.42
HadRM3H	3.38	4.24	4.28	4.46	4.87	4.76	4.64	4.63
RegCM	3.04	3.83	3.87	4.01		4.17	4.29	4.24
RACMO	2.91	4.07	3.55	3.53	4.02	3.97	4.31	3.98
REMO	3.01	4.18	3.98	3.80	4.47	4.16	4.15	4.07
RCAO-50	3.04	3.96	4.12	4.13	4.27	4.25	4.29	4.27
RCAO-25	3.08	4.00	4.17	4.14	4.28	4.41	4.24	4.28
PROMES	2.95	4.21	3.88	3.94		4.31	4.33	4.23
HadAM3H	3.33	4.41	4.19	4.45	4.96	4.66	4.80	4.93
ARPEGE	2.69	3.88	3.63	3.86	3.82	3.82	4.24	4.61
HIRHAM-ECH	4.15	5.43	5.41	5.30	5.29	5.69	5.29	5.85
RCAO-ECH	4.01	5.54	5.40	5.14	4.66	5.35	4.88	5.29
Ensemble	3.01	3.96	3.83	3.85	4.36	4.15	4.20	4.09

Table 3 Relative change in seasonal mean precipitation for the 8 areas under investigation

DJF	BI	IP	FR	ME	SC	AL	MD	EA
HIRHAM-50	0.15	-0.02	0.26	0.21	0.23	0.24	0.01	0.24
HIRHAM-25	0.17	-0.02	0.27	0.21	0.24	0.21	0.03	0.23
HIRHAM-12	0.18	-0.02	0.28	0.24	0.22	0.24	0.03	0.24
CHRM	0.19	-0.08	0.23	0.15	0.22	0.21	-0.01	0.21
CLM	0.22	-0.04	0.26	0.18	0.22	0.21	0.06	0.27
HadRM3H	0.17	-0.08	0.18	0.14	0.18	0.19	-0.06	0.16
RegCM	0.23	-0.01	0.23	0.18		0.16	0.00	0.23
RACMO	0.19	-0.05	0.24	0.15	0.20	0.22	-0.02	0.22
REMO	0.25	-0.04	0.24	0.14	0.22	0.23	-0.07	0.17
RCAO-50	0.18	-0.02	0.23	0.21	0.23	0.21	-0.02	0.25
RCAO-25	0.18	-0.01	0.24	0.24	0.23	0.26	0.01	0.26
PROMES	0.21	-0.02	0.23	0.15		0.19	0.01	0.20
HadAM3H	0.18	-0.03	0.20	0.15	0.21	0.19	-0.00	0.20
ARPEGE	0.17	-0.01	0.20	0.16	0.20	0.11	-0.08	0.11
HIRHAM-ECH	0.13	0.03	0.07	0.18	0.35	0.05	-0.07	0.19
RCAO-ECH	0.29	-0.07	0.16	0.34	0.54	0.05	-0.27	0.16
Ensemble	0.20	-0.04	0.23	0.17	0.21	0.20	-0.01	0.22

MAM	BI	IP	FR	ME	SC	AL	MD	EA
HIRHAM-50	0.02	-0.28	-0.03	0.08	0.11	0.03	-0.10	0.06
HIRHAM-25	0.03	-0.28	-0.01	0.10	0.10	0.08	-0.05	0.11
HIRHAM-12	0.04	-0.27	0.02	0.12	0.10	0.08	-0.05	0.10
CHRM	0.03	-0.39	-0.04	0.03	0.12	-0.04	-0.15	-0.01
CLM	0.05	-0.29	0.03	0.07	0.15	0.07	-0.10	0.01
HadRM3H	-0.01	-0.29	-0.09	0.07	0.11	-0.00	-0.17	-0.02
RegCM	0.07	-0.27	-0.04	0.08		0.04	-0.12	0.09
RACMO	0.04	-0.32	-0.01	0.12	0.13	0.03	-0.14	-0.01
REMO	0.03	-0.31	-0.05	0.08	0.09	0.01	-0.09	0.06
RCAO-50	0.07	-0.28	-0.01	0.13	0.18	0.01	-0.11	0.04
RCAO-25	0.09	-0.29	0.01	0.12	0.18	0.02	-0.07	0.10
PROMES	0.07	-0.28	-0.03	0.19		0.06	-0.12	0.13
HadAM3H	0.02	-0.31	-0.04	0.05	0.12	0.02	-0.12	-0.00
ARPEGE	0.11	-0.24	-0.06	0.06	0.19	-0.10	-0.29	0.06
HIRHAM-ECH	-0.04	-0.26	-0.23	-0.11	0.23	-0.15	-0.21	-0.01
RCAO-ECH	0.05	-0.50	-0.36	-0.09	0.43	-0.29	-0.43	-0.10
Ensemble	0.04	-0.30	-0.03	0.09	0.13	0.02	-0.12	0.04

JJA	BI	IP	FR	ME	SC	AL	MD	EA
HIRHAM-50	-0.35	-0.39	-0.34	-0.20	-0.02	-0.20	-0.30	-0.21
HIRHAM-25	-0.28	-0.38	-0.31	-0.16	0.04	-0.20	-0.31	-0.17
HIRHAM-12	-0.26	-0.36	-0.28	-0.16	0.04	-0.18	-0.31	-0.13
CHRM	-0.36	-0.72	-0.55	-0.23	0.03	-0.41	-0.64	-0.23
CLM	-0.33	-0.46	-0.43	-0.25	0.06	-0.25	-0.46	-0.19
HadRM3H	-0.39	-0.44	-0.51	-0.32	-0.02	-0.31	-0.44	-0.28
RegCM	-0.30	-0.39	-0.41	-0.17		-0.17	-0.35	-0.06
RACMO	-0.33	-0.60	-0.45	-0.22	-0.03	-0.34	-0.68	-0.31
REMO	-0.36	-0.50	-0.39	-0.15	0.19	-0.17	-0.28	0.02
RCAO-50	-0.35	-0.50	-0.52	-0.27	-0.01	-0.39	-0.57	-0.23
RCAO-25	-0.33	-0.49	-0.42	-0.21	0.04	-0.36	-0.48	-0.12
PROMES	-0.22	-0.45	-0.37	-0.05		-0.18	-0.42	0.05
HadAM3H	-0.35	-0.44	-0.50	-0.32	-0.02	-0.33	-0.45	-0.28
ARPEGE	-0.16	-0.48	-0.33	-0.14	0.11	-0.19	-0.31	-0.17
HIRHAM-ECH	-0.19	-0.26	-0.38	-0.30	-0.07	-0.21	-0.21	-0.23
RCAO-ECH	-0.29	-0.43	-0.63	-0.48	-0.00	-0.44	-0.41	-0.39
Ensemble	-0.33	-0.48	-0.43	-0.21	0.03	-0.26	-0.43	-0.15

SON	BI	IP	FR	ME	SC	AL	MD	EA
HIRHAM-50	-0.02	-0.17	-0.12	-0.09	0.04	-0.10	-0.10	-0.09
HIRHAM-25	-0.01	-0.17	-0.08	-0.04	0.08	-0.11	-0.12	-0.04
HIRHAM-12	0.00	-0.16	-0.08	-0.03	0.09	-0.09	-0.10	-0.03
CHRM	-0.00	-0.26	-0.15	-0.10	0.01	-0.08	-0.12	-0.17
CLM	-0.03	-0.20	-0.14	-0.08	0.06	-0.05	0.03	-0.06
HadRM3H	-0.05	-0.19	-0.13	-0.11	-0.01	-0.13	-0.11	-0.13
RegCM	-0.02	-0.12	-0.09	0.02		-0.02	-0.09	-0.04
RACMO	0.02	-0.21	-0.11	-0.04	0.03	-0.05	-0.12	-0.09
REMO	-0.07	-0.23	-0.13	-0.11	0.07	-0.07	0.00	-0.09
RCAO-50	-0.02	-0.17	-0.09	-0.06	0.06	-0.10	-0.18	-0.08
RCAO-25	-0.00	-0.16	-0.10	-0.04	0.07	-0.07	-0.13	-0.08
PROMES	0.01	-0.16	-0.12	-0.01		0.01	-0.07	-0.06
HadAM3H	-0.06	-0.20	-0.13	-0.07	-0.01	-0.06	-0.10	-0.10
ARPEGE	0.17	-0.25	0.03	0.08	0.20	-0.02	-0.12	-0.08
HIRHAM-ECH	0.04	-0.25	-0.18	-0.02	0.26	-0.13	-0.12	-0.06
RCAO-ECH	0.11	-0.33	-0.12	0.05	0.29	-0.12	-0.20	0.03
Ensemble	-0.02	-0.19	-0.12	-0.06	0.04	-0.07	-0.08	-0.09

List of figures

Figure 1: Diagram explaining the organisation of the individual model experiments. The black frame indicates the nine RCM experiments in the standard ensemble.

Figure 2a: Temperature Change [°C] DJF, cf. Figure 1. The standard deviation has been scaled by a factor of 10.

Figure 2b: Temperature Change [°C] JJA, cf. Figure 1. The standard deviation has been scaled by a factor of 10.

Figure 3a: Precipitation change [%] DJF, cf. Figure 1. The standard deviation has been scaled by a factor of 10.

Figure 3b: Precipitation change [%] JJA, cf. Figure 1. NOTE: The standard deviation has been scaled by a factor of 5.

Figure 4: European sub-areas

Figure 5: A schematic overview of seasonal changes as simulated by the PRUDENCE regional models. In each panel, rows are the analysis areas, columns correspond to models. Rows of panels signify the four seasons, the left column of panels are temperature change (left color bar, degrees C), whereas the right column of panels signifies precipitation (right color bar, relative change). Areas not covered by a particular model are indicated by black squares.

Figures

Figure 1: Diagram explaining the organisation of the individual model experiments. The black frame indicates the nine RCM experiments in the standard ensemble. Leftmost column and bottom row indicate coordinates as used in the text, e.g. the panel with Observed CRU is referred to as 1A.

	A	B	C	D
1	Observed CRU		Ensemble mean from standard experiments	Ensemble standard deviation of standard experiments
2	HadAM3H Ensemble member 1 Driving model for standard RCM experiments	HadRM3H Ensemble member 1	HadRM3P Ensemble member 1	HadAM3P Ensemble member 1 Driving model for HadRM3P experiments
3	CHRM	CLM	RegCM	RACMO
4	REMO	PROMES	RCAO	HIRHAM Ensemble member 1
5			RCA2 25km	HIRHAM 25km
6	HadCM3 Ensemble member 1	ARPEGE Ensemble member 1 SSTs as for standard RCM experiments		HIRHAM 12km
7		ARPEGE SSTs taken from experiment using ARPEGE/OPA	RCAO ECHAM4/OPYC3 boundaries	HIRHAM ECHAM4/OPYC3 boundaries

Figure 2a: Temperature Change [°C] DJF, cf. Figure 1. The standard deviation has been scaled by a factor of 10.

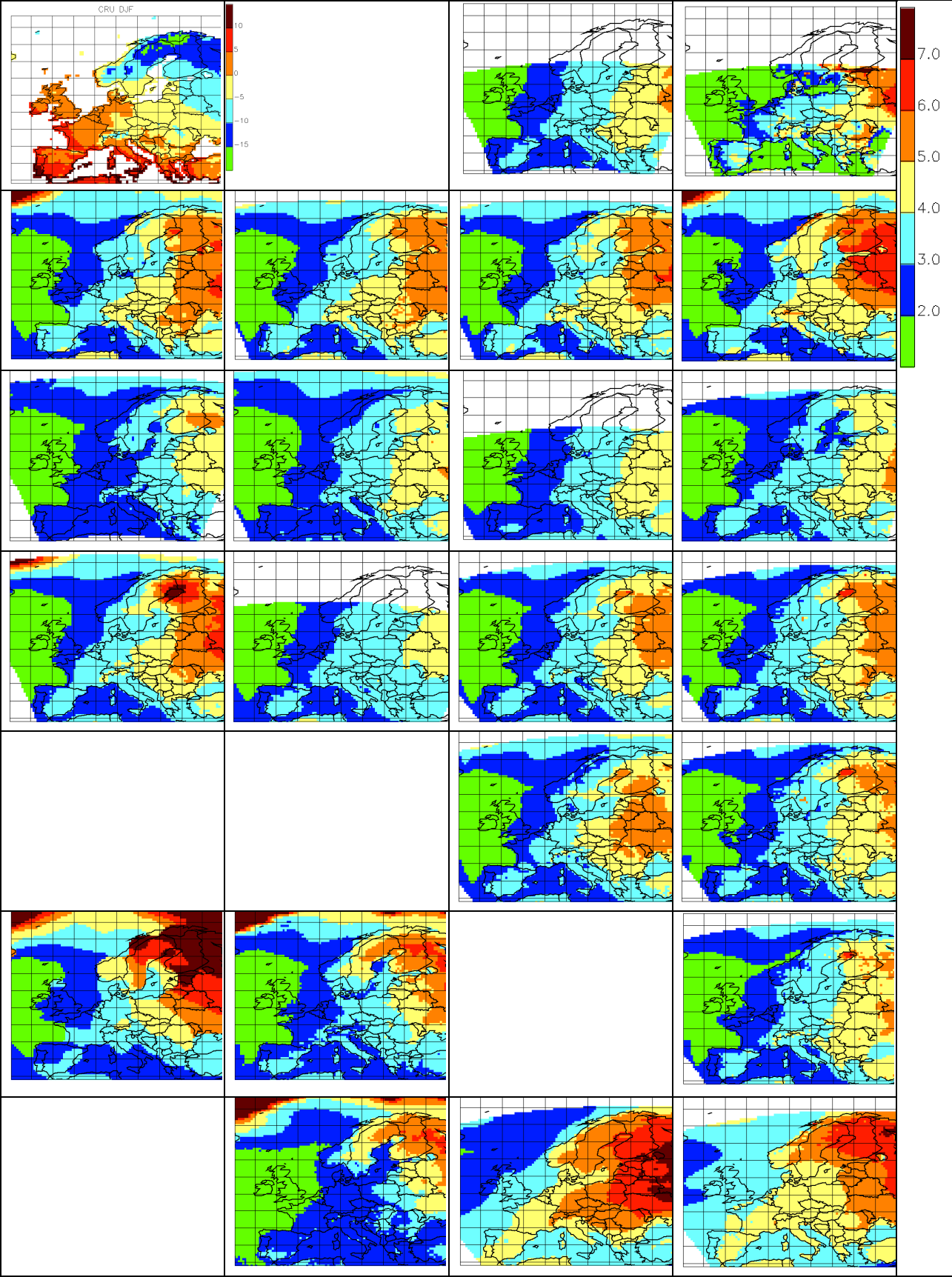


Figure 2b: Temperature Change [°C] JJA, cf. Figure 1. The standard deviation has been scaled by a factor of 10.

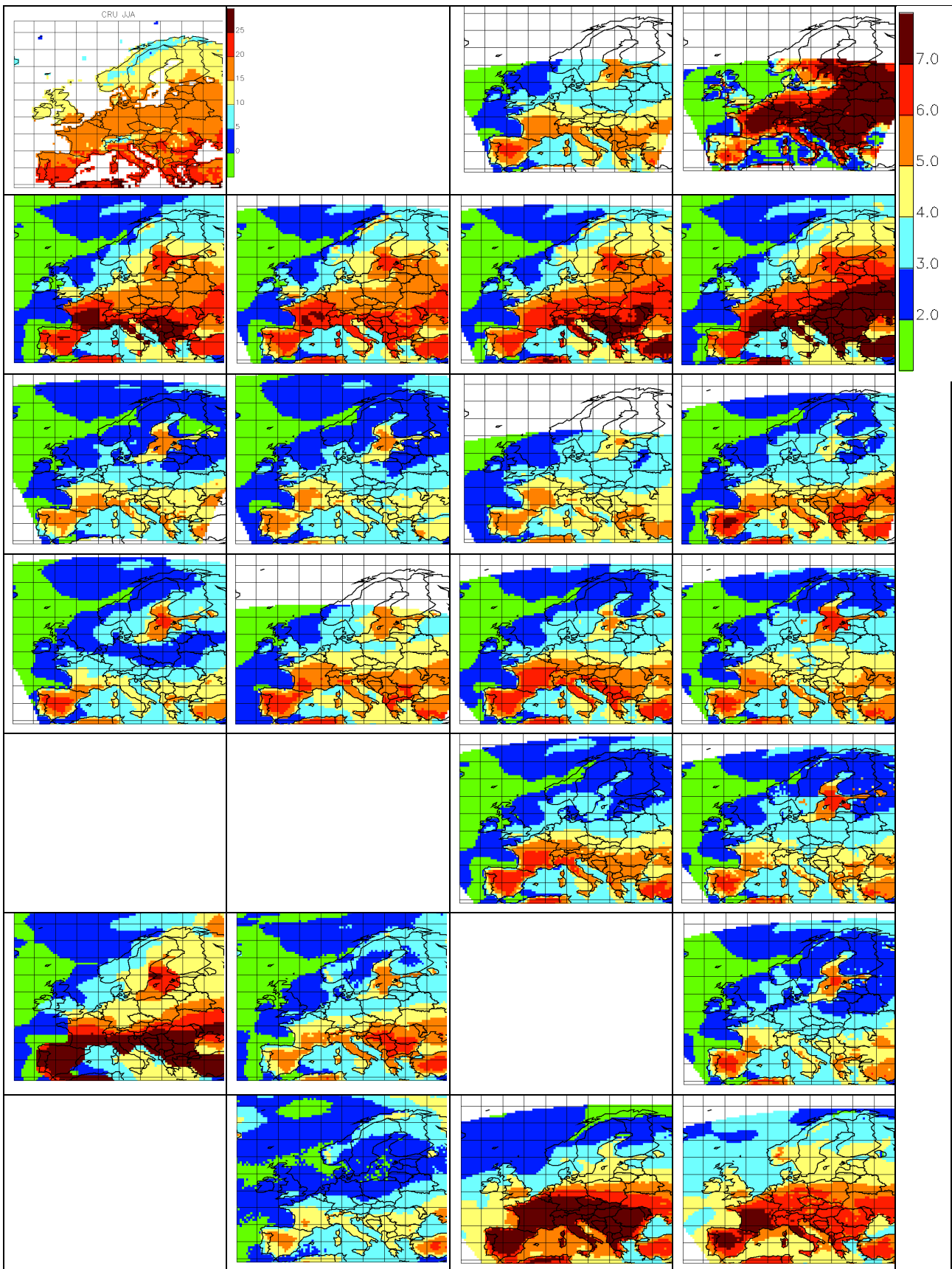


Figure 3a: Precipitation change [%] DJF, cf. Figure 1. The standard deviation has been scaled by a factor of 10.

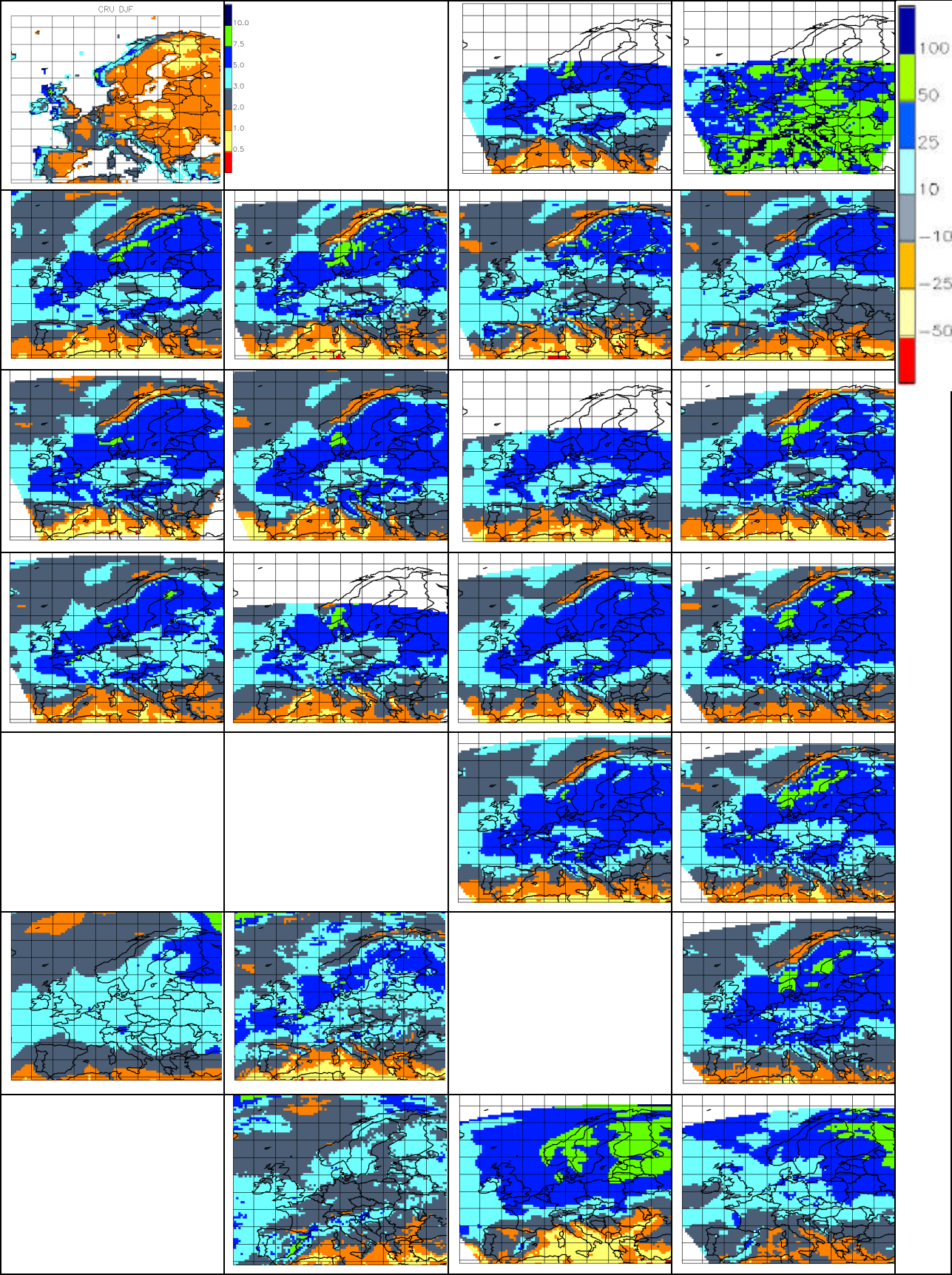


Figure 3b: Precipitation change [%] JJA, cf. Figure 1. NOTE: The standard deviation has been scaled by a factor of 5.

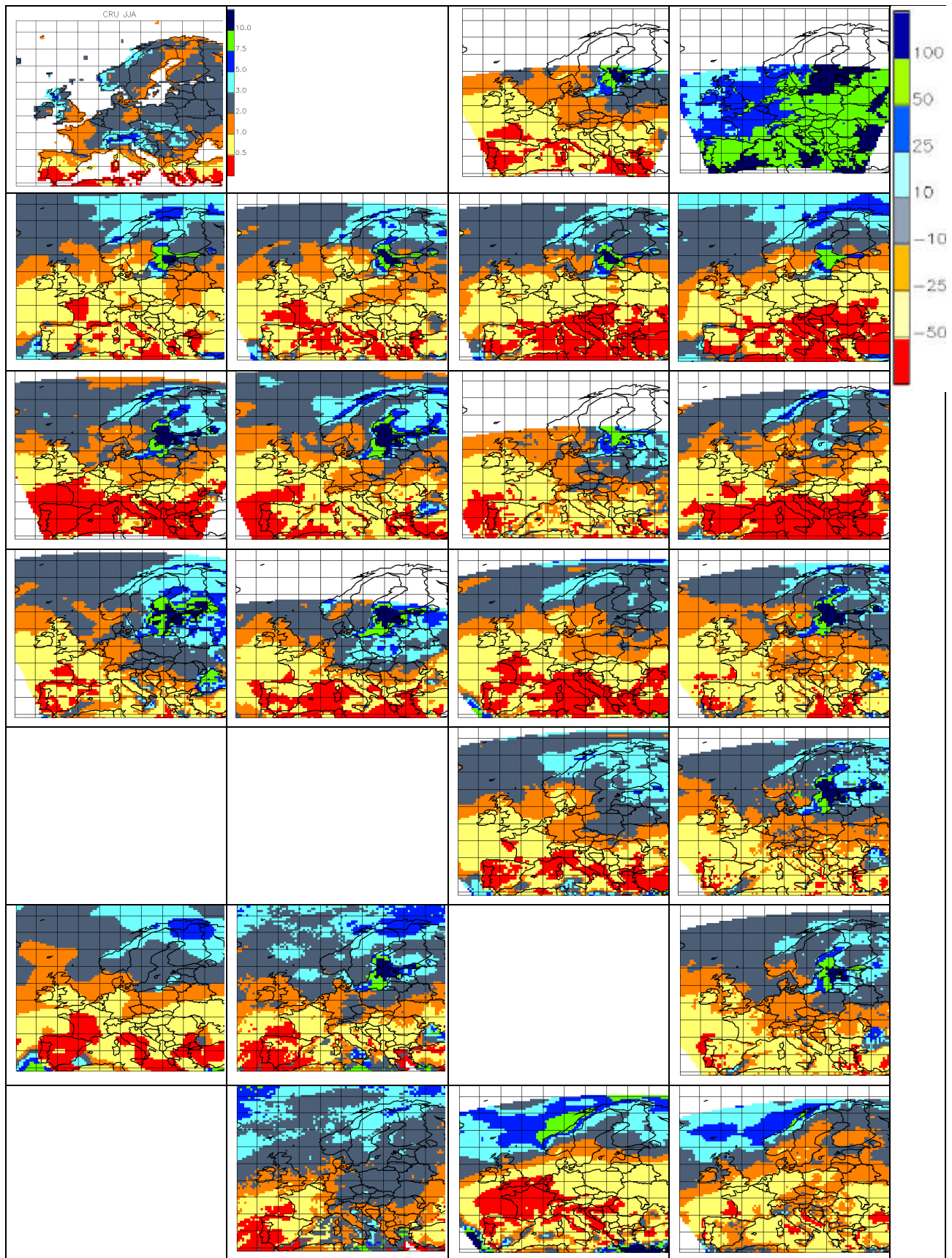


Figure 4: European sub-areas

Area	West	East	South	North
1 (BI) British Isles	-10	2	50	59
2 (IP) Iberian Peninsula	-10	3	36	44
3 (FR) France	-5	5	44	50
4 (ME) Mid-Europe	2	16	48	55
5 (SC) Scandinavia	5	30	55	70
6 (AL) Alps	5	15	44	48
7 (MD) Mediterranean	3	25	36	44
8 (EA) Eastern Europe	16	30	44	55

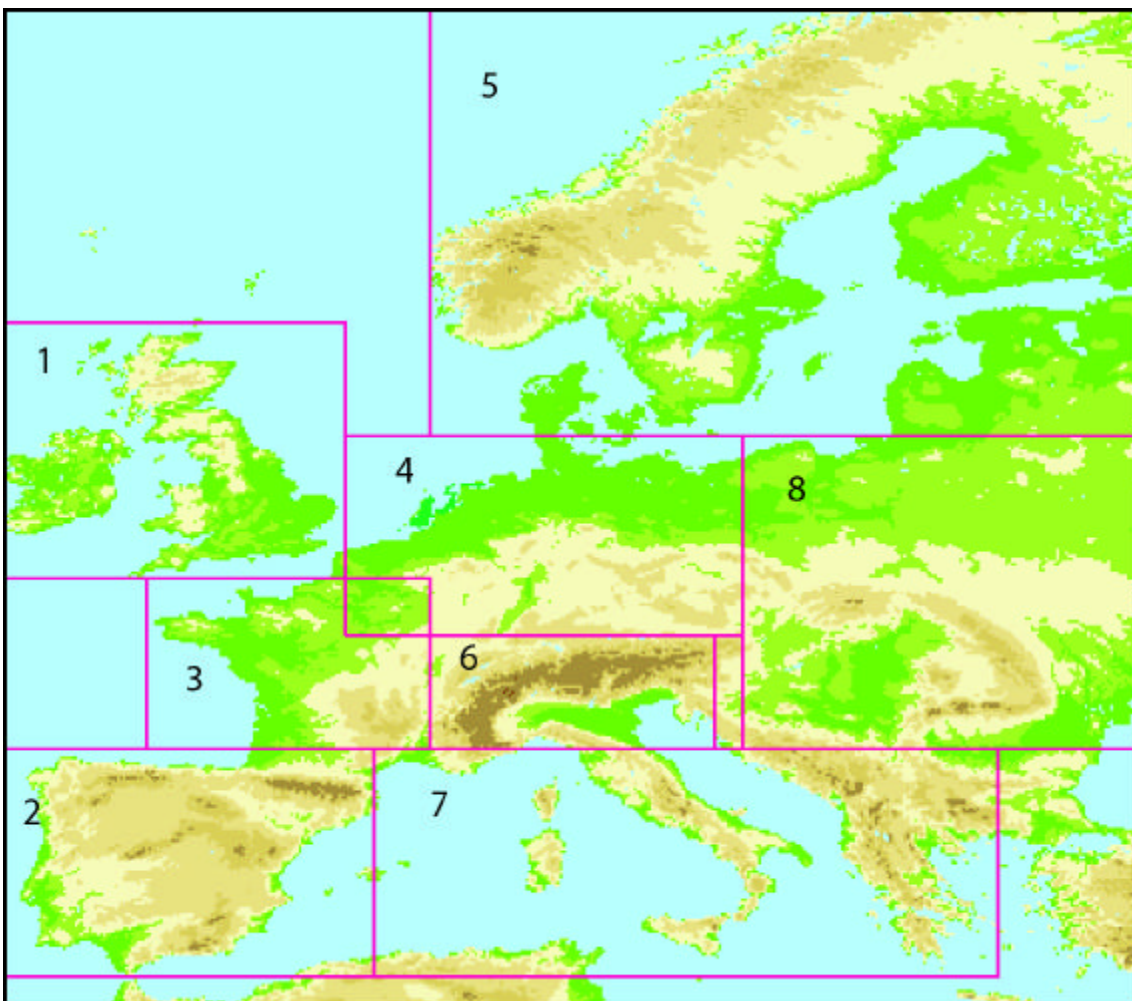


Figure 5: A schematic overview of seasonal changes as simulated by the PRUDENCE regional models. In each panel, rows are the analysis areas, columns correspond to models. Rows of panels signify the four seasons, the left column of panels are temperature change (left color bar, degrees C), whereas the right column of panels signifies precipitation (right color bar, relative change). Areas not covered by a particular model are indicated by black squares.

